HHS Public Access

Author manuscript

Sci Transl Med. Author manuscript; available in PMC 2017 August 04.

Published in final edited form as:

Sci Transl Med. 2017 January 04; 9(371): . doi:10.1126/scitranslmed.aah3532.

Optimized temporal pattern of brain stimulation designed by computational evolution

David T. Brocker[1], **Brandon D. Swan**[1], **Rosa Q. So**[1], **Dennis A. Turner**[2,3], **Robert E. Gross**[4,5], and **Warren M. Grill**[1,2,*]

[1]Department of Biomedical Engineering, Duke University, Durham, NC 27708

[2]Department of Neurobiology, Duke University Medical Center, Durham, NC 27710

[3]Department of Neurosurgery, Duke University Medical Center, Durham, NC 27710

[4]Department of Neurosurgery and Neurology, Emory University, Atlanta, GA 30322

[5]Coulter Department of Biomedical Engineering, Georgia Institute of Technology, Atlanta, GA 30332

Abstract

Brain stimulation is a promising therapy for several neurological disorders, including Parkinson's disease. Stimulation parameters are selected empirically and are limited to the frequency and intensity of stimulation. We used the temporal pattern of stimulation as a novel parameter of deep brain stimulation to ameliorate symptoms in a parkinsonian animal model and in humans with Parkinson's disease. We used model-based computational evolution to optimize the stimulation pattern. The optimized pattern produced symptom relief comparable to that from standard high-frequency stimulation (a constant rate of 130 or 185 Hz) and outperformed frequency-matched standard stimulation in the parkinsonian rat and in patients. Both optimized and standard stimulation suppressed abnormal oscillatory activity in the basal ganglia of rats and humans. The results illustrate the utility of model-based computational evolution to design temporal pattern of stimulation to increase the efficiency of brain stimulation in Parkinson's disease, thereby requiring substantially less energy than traditional brain stimulation.

Introduction

Parkinson's disease (PD) is a progressive, neurodegenerative disease characterized by motor symptoms that include bradykinesia, resting tremor, postural instability, and rigidity (1, 2). Although dopamine replacement therapy treats the symptoms of PD, long-term use is

*To whom correspondence should be addressed: warren.grill@duke.edu.

Author contributions: D.T.B. and W.M.G. designed research; D.T.B., B.D.S., R.Q.S., D.A.T., R.E.G. and W.M.G. performed research; D.T.B. and W.M.G. analyzed data and wrote the paper.

Competing interests: D.T.B. and W.M.G. are inventors on patent applications related to non-regular patterns of DBS and hold equity in Deep Brain Innovations, LLC, which has licensed intellectual property from Duke University. R.E.G. receives research funding from Medtronic; he also serves as a consultant to Medtronic and receives compensation for these services. The terms of this arrangement have been reviewed and approved by Emory University in accordance with its conflict of interest policies.

Data and materials availability: Experimental results in individual animals and human subjects are provided in Supplementary Material.

complicated by the requirement for higher and more frequent dosing, motor fluctuations, and dyskinesias (3). Deep brain stimulation (DBS) is an effective and adjustable surgical treatment for advanced PD (4, 5) that improves motor symptoms, improves quality of life, and reduces motor fluctuations (6). However, this therapy has not been optimized, and there have been few improvements in DBS since its introduction.

The stimulation parameters used for DBS are determined empirically and consist of short-duration (60–180 μs), high-frequency (typically 130–185 Hz) pulses of electrical stimulation to ameliorate symptoms (7–9). The efficacy of DBS is strongly dependent on the frequency of stimulation: low-frequency stimulation (< 50 Hz) is ineffective or exacerbates symptoms, while high-frequency stimulation produces symptomatic benefit. Nevertheless, high stimulation frequencies can cause stronger side effects (10, 11) and consume more energy (12) than low frequency stimulation, leading to frequent surgical replacement of battery-powered, implanted pulse generators (IPGs) (13). IPG replacement surgeries are expensive and carry risks, including infection and mis-programming (14).

Present DBS systems deliver a regular temporal pattern of stimulation; interpulse intervals do not vary as a function of time. Irregular temporal patterns of stimulation have been used in animal (15–17) and human studies (18–22) to probe DBS mechanisms. Random patterns of DBS, even when delivered at a high average frequency, are not effective in ameliorating parkinsonian symptoms in rats (17), tremor in persons with essential tremor (21, 22) or bradykinesia in patients with PD (18). These results indicate that the effects DBS on symptoms are strongly dependent on the temporal pattern of stimulation and motivated our current study in which we sought to design a temporal pattern for DBS that would be more efficient than conventional high-frequency DBS.

Results

Design of optimized temporal pattern of stimulation with computational evolution

We used model-based computational evolution to design an optimized temporal pattern of stimulation that reduced the average stimulation frequency of DBS and preserved efficacy (thereby reducing the energy requirement for stimulation and consequent risks associated with frequent IPG replacements). A model of the basal ganglia was coupled with a genetic algorithm and used in the design of optimized stimulation pattern. Genetic algorithms (GA) are well suited to this problem, where there is a highly complex, non-linear relationship between the input (stimulus pattern) and output (neural activity), and the GA operates analogously to evolution through natural selection, where the organisms are the temporal patterns of DBS. The GA was used to design a stimulation pattern that minimized average stimulation frequency and error index (EI), a model-based proxy for symptoms (Fig. 1A). The EI is a measure of the fidelity of information transmission through the thalamus under modulation by the output of the basal ganglia (23), and was used here as a proxy for parkinsonian bradykinesia (18) (Fig. 1B). The fitness of each stimulation pattern was evaluated with a cost function that incentivized reducing both EI and the average stimulation frequency. Patterns with greater fitness were more likely to pass their genes (pattern characteristics) on to the next generation of patterns (Fig. 1, C and D). The cost of the best stimulation pattern in each generation declined monotonically across generations, while the

median cost across the population in each generation declined more slowly (Fig. 1E). The resulting optimal pattern had an average frequency of 45 Hz and reduced the EI in the model by almost 98% relative to a 45 Hz, constant-frequency stimulation (Fig. 1F).

Efficacy of optimized GA pattern of stimulation in hemi-parkinsonian rats

The optimized pattern of DBS (GA) was compared to DBS-off (baseline), 45 Hz DBS, and 130 Hz DBS in hemi-parkinsonian rats by using two well-established measures of parkinsonian symptoms that exhibit DBS frequency-dependent effects that parallel those observed in clinical studies (24): the bar test to assess akinesia (Fig. 2A) and methamphetamine-induced circling to assess locomotor behavior (Fig. 2B).

There was a significant effect of stimulation condition on time on the bar, and all patterns of stimulation reduced time on the bar compared to baseline. Both 130 Hz and GA significantly reduced time on the bar compared to 45 Hz (Fig. 2C). Similarly, there was a significant effect of stimulation condition on circling rate, and all patterns of DBS reduced circling rate compared to baseline. High-frequency (130 Hz) DBS reduced circling rate more completely than did 45 Hz or GA. Although in humans with PD, <50 Hz DBS is ineffective and 130–185 Hz is used for treatment, in 6-hydroxydopamine (6-OHDA) lesioned rats DBS at 30–75 Hz is at least partially effective at treating parkinsonian symptoms including methamphetamine-induced circling (24, 25), akinesia (24), and reduced open field mobility (26). Thus, in parkinsonian rats, the optimized GA stimulation pattern performed better than the partially effective standard 45 Hz, although 130 Hz DBS performed better than either. There was no effect of stimulation condition on normalized distance traveled (Fig. S1); the results from this control indicate that the reductions in circling rate achieved by DBS (Fig 2D) did not simply reflect decreases in overall movement or activity, but rather demonstrate a resolution of the pathological circling behavior (25).

Efficacy of optimized pattern of stimulation in subjects with PD

We quantified unilateral motor symptoms—either bradykinesia or tremor—on the more affected side in subjects with STN DBS for PD (Table 1) undergoing IPG replacement surgery during DBS off (baseline), temporally regular 185 Hz DBS (185 Hz), temporally regular 45 Hz DBS (45 Hz), and the optimized GA pattern with an average frequency of 45 Hz (GA).

We tested bradykinesia-dominant PD subjects (n=4) with an alternating finger tapping task (27), a quantitative outcome measure strongly correlated with clinical measures of bradykinesia (20, 27) (Fig. 3, A and B). There was a significant effect of stimulation condition on the rate (Fig. S2) and regularity (Fig. 3C) of finger tapping. Both GA and 185 Hz significantly improved both the rate and regularity of finger tapping compared to baseline, but 45 Hz only improved tapping rate. Tapping variability was not different between GA and 185 Hz, and both were lower than 45 Hz.

We exploited the correlation between the regularity of finger tapping and Unified Parkinson's Disease Rating Scale (UPDRS) Part III motor examination sub-scores (20, 27) to estimate the clinical impact of the different patterns of stimulation. The finger tapping data suggested that 185 Hz reduced UPDRS motor scores by nearly 34 points on average

compared to baseline (Fig. 3D), consistent with previously described effects of DBS (28), while GA was predicted to reduce UPDRS motor scores by 31 points. Both GA and 185 Hz were predicted to reduce UPDRS motor scores over 12 points more on average than 45 Hz.

We quantified unilateral tremor in tremor-dominant PD subjects (n=4) using an accelerometer attached to the dorsum of the hand (Fig. 4). There was a significant effect of DBS pattern on tremor (Fig. 4C). Tremor was decreased significantly compared to baseline by GA and 185 Hz. However, 45 Hz did not alter tremor relative to baseline. Further, GA and 185 Hz both significantly decreased tremor compared to 45 Hz.

We used the logarithmic relationship (29) between tremor amplitude and a clinical tremor rating scale (TRS; 0=no tremor to 4=severe tremor) to estimate the clinical and functional impact of the patterns of DBS on tremor. The no-stimulation and 45 Hz conditions reduced the estimated TRS score by less than one point, while GA reduced estimated TRS score by about two points and 185 Hz eliminated tremor (Fig. 4D). These data indicate that 185 Hz effectively suppressed tremor of all magnitudes, while GA suppressed completely only less-severe tremor. Indeed, GA DBS effectively suppressed tremor in two tremor-dominant PD subjects with a mean baseline tremor power of 61.5 m^2/s^4, but did not suppress tremor in two subjects with a mean baseline tremor power of 153 m^2/s^4.

Optimized pattern of DBS suppresses low frequency oscillations

We hypothesized that the efficacy of temporal patterns of brain stimulation may be related to the suppression of the low frequency oscillatory neural activity that is prevalent in PD (30) and in animal models of PD (24). Hemi-parkinsonian rats exhibit exaggerated 7–10 Hz oscillations that are suppressed in a stimulation frequency-dependent manner, similar to the frequency-dependent amelioration of clinical motor symptoms (11, 24, 31, 32). We recorded field potentials from motor cortex and globus pallidus (GP) ipsilateral to the dopaminergic lesion and STN stimulating electrodes and quantified suppression of 7–10 Hz oscillations in hemi-parkinsonian rats during stimulation with each pattern. We observed a significant effect of DBS pattern on 7–10 Hz power in both GP and ipsilateral motor cortex. Low frequency oscillatory power was significantly lower during GA and 130 Hz than during 45 Hz in both GP and motor cortex (Fig. 5).

Human subjects with PD exhibit exaggerated β-band oscillations (30), and improvements in bradykinesia after dopamine therapy and high frequency DBS are associated with reductions in this β activity (33). We quantified β-band power across stimulation patterns in six human subjects undergoing surgical implantation of the DBS lead in STN for PD. β-band power was prominent in the DBS off condition and was suppressed differentially by the stimulation patterns (Fig. 6A). GA and 130 Hz both significantly suppressed β-band power compared to the off condition and 45 Hz (Fig. 6B). β-power from this cohort of DBS implant subjects was correlated, across DBS conditions, with the finger tapping performance that we measured in the earlier cohort of subjects undergoing motor symptom measurement (Fig. 6C).

Discussion

We combined model-based optimization using computational evolution, preclinical experiments in a parkinsonian animal model, and translational experiments in patients with PD to design and evaluate a new temporal pattern of DBS. The optimized temporal pattern achieved efficacy at a low average frequency that was not effective during non-patterned stimulation. Further, the suppression of low frequency oscillations by both the GA and high frequency DBS suggests a potential therapeutic mechanism shared by effective stimulation, whether patterned or un-patterned. Although there is a correlation between β-frequency power and bradykinesia (34, 35) and β activity is suppressed by DBS and levodopa (36), β activity does not correlate consistently with motor symptoms (37) and changes in β activity are inconsistent across patients (38, 39). Therefore, it remains unclear to what degree suppression of β activity can serve as an index of therapeutic efficacy.

We designed and evaluated a procedure to optimize temporal patterns of neural stimulation to maximize simultaneously efficacy and efficiency. The pattern of DBS emerging from our computational evolution method was only optimal for the specific model and cost function that were used, and it may be possible to improve further the efficacy and efficiency of non-regular patterns of stimulation in a patient-specific manner, for example, by building patient-specific models for optimization.

Our optimized temporal pattern of stimulation that produced symptom relief at a lower average frequency has advantages over conventional high frequency DBS (typically 130 – 185 Hz). IPGs delivering the optimized low frequency pattern of stimulation will consume less energy (12), and reduced energy consumption translates into longer battery life and less frequent IPG replacement (13, 40). We estimated that the subjects included in this study would achieve an average of 3.9 years of additional battery life had they used GA DBS instead of their current high frequency DBS (Fig. S3). In contrast to previous work using DBS at frequencies less than 100 Hz (41), the stimulation pulse width and amplitude in our study were identical to those used for high frequency stimulation, but the optimized temporal (GA) pattern delivered substantially less electrical energy (12). Lower average stimulation frequencies may also decrease stimulation side effects, as there is an inverse relationship between stimulation frequency and side effect intensity (10, 11). However, the nature of the intraoperative testing environment precluded assessment of the effect of stimulation pattern of the side effects produced by DBS. Intermittent DBS may be an alternative approach to reduce stimulation energy, but intermittent thalamic stimulation in patients with essential tremor (42, 43) and intermittent STN DBS in patients with PD (19) were less effective than constant stimulation.

The short duration of DBS and assessment of symptoms is a limitation of our studies. Although, similar trial lengths are used in studies of parameter settings (11, 32) and for intraoperative testing and post-operative tuning, they may be too short to enable full development of the effects of stimulation. Tremor reduction after onset of DBS and recovery after cessation of DBS occurs within seconds (21, 44, 45), and approximately 85 % of the reduction of bradykinesia occurs within 2 min of starting DBS (46). Our short trials may

have underestimated the changes in symptoms, but this underestimation would be similar across stimulation patterns and therefore allow valid relative comparisons.

The GA DBS performance was equivalent to high frequency DBS in the bradykinesia-related finger tapping task. The predicted changes in UPDRS motor subscores produced by stimulation with the GA pattern were equivalent to those produced by 185 Hz, comparable to those in large, randomized trials of DBS (47–49), and exceeded the threshold for large clinically important differences (50, 51). This suggests that GA and 185 Hz DBS will provide functionally similar alleviation of motor symptoms and clinically meaningful symptom improvement in bradykinesia-dominant PD patients. The suppression of parkinsonian tremor by GA DBS was somewhat lower than high frequency DBS, suggesting that our GA DBS pattern may be most appropriate for patients with mild tremor whose primary symptom is bradykinesia. The differential effect on symptoms was consistent with the relationship between EI, used as a model-based proxy for symptoms during the design process, and bradykinesia observed in previous clinical experiments (18), and points to an opportunity for optimizing tremor-specific temporal patterns of stimulation by using a tremor-related outcome measure in the computational model.

One of the desired outcomes from a closed-loop DBS system for PD and other neurological disorders (16, 52, 53) is energy savings due to the demand-controlled stimulation. However, the energy required for feedback signal amplification, acquisition, and processing may mitigate possible energy savings from demand-controlled stimulation. As well, this approach is currently hindered by difficulty selecting and recording a symptom-relevant biomarker. Conversely, non-regular temporal patterns of DBS with a low average frequency can provide substantial increases in energy efficiency while bypassing challenges associated with closed-loop systems.

Materials and Methods

Study Design

The aim of this study was to design an optimized pattern of DBS (GA) and evaluate its efficacy and mechanisms in hemi-parkinsonian rats and human subjects with PD. Our hypothesis, based on the computational modeling results, was that GA would reduce motor symptoms in hemi-parkinsonian rats and human subject with PD to the same extent as regular high-frequency stimulation. Rat behavioral experiments were designed on the basis of power analyses that indicated that ten rats would reveal differences between effective and ineffective stimulation patterns. We projected enrollment numbers of subjects with Parkinson’s disease based on a previous study, but as an exploratory proof-of-concept study and acute intervention, we did not have explicit stoppage or endpoint criteria. The order of stimulation pattern presentation was randomized across all experiments in rats and humans, and pre-defined quantitative measures of motor performance were used to assess parkinsonian symptoms.

Computation Model of the Basal Ganglia

Temporal patterns of DBS were designed using a biophysical network model of the basal ganglia and thalamus in the PD state. The model was modified from the original version (23) to represent better neural activity and effects of DBS in PD (54). The model included 10 neurons in each of the external globus pallidus (GPe), subthalamic nucleus (STN), internal globus pallidus (GPi), and thalamus (TH). The single compartment model neurons received constant applied currents to represent putative afferent projections that maintained average firing rates consistent with observations in non-human primate models of PD and humans with PD (55–58). Thalamic neurons did not receive constant applied currents, but rather received excitatory pulse inputs, intended to represent action potentials from the sensorimotor cortex, that arrived at a frequency of 14 Hz (±20%). EI was calculated by quantifying the fidelity of the thalamic neurons' responses to these inputs. STN DBS was applied by delivering the pattern of current pulses to each STN neuron. Model simulations were implemented in MATLAB using the forward Euler method with a time step of 0.01 ms and a total simulated time of 50 s.

Stimulation Pattern Design Using a Genetic Algorithm

A genetic algorithm is an optimization technique based on principles from biological evolution (62). Patterns of stimulation were encoded using bit strings. Each bit in the string represented 1 ms of time, and the bit's value indicated whether a DBS current pulse was present (1) or not (0) in that epoch. Bit strings contained 200 elements, making each pattern 200 ms long. During initial testing of the GA, we employed an iterative empirical process to identify an appropriate pattern length; longer pattern lengths required many more generations to converge, while patterns that were too short did not result in optimal solutions. To evaluate the DBS patterns in the model, the 200 ms repeating pattern was applied to the STN neurons. After a random initial population of patterns was generated, patterns were evaluated using a cost function and "mated" to create a new population/generation of patterns. After 90 generations, the optimized pattern of stimulation was selected for testing in hemi-parkinsonian rats and patients with PD. The resulting optimal pattern was a repeating vector of interpulse intervals, in ms, [2 50 16 4 52 19 2 48 7]. Multiple iterations of the optimization algorithm yielded highly reproducible temporal patterns.

Each pattern's performance in the computational model was calculated using a cost function,

$$Cost = 100\% * \frac{EI_{pattern} - EI_{FMC}}{EI_{FMC}},$$

where $EI_{pattern}$ was the pattern's EI, and EI_{FMC} was the EI of the pattern's frequency-matched regular DBS control pattern. Therefore, the cost function was the percent change in EI compared to the pattern's frequency-matched regular DBS control. Since high-frequency regular DBS was highly effective in the model (23, 54), this cost function incentivized low average frequency patterns of stimulation that suppressed errors in the model without explicitly including stimulation frequency in the cost function.

Several lines of evidence support the use of the thalamic relay EI as a model-based proxy for parkinsonian symptoms. Changes in EI as a function of DBS frequency (54) parallel changes in parkinsonian symptoms in 6-OHDA lesioned rats during different frequencies of STN DBS (24). Similarly, there is a strong correlation between the EI in the model and bradykinesia in persons with PD across different random temporal patterns of DBS (18). As well, driving the model with GPi activity recorded from parkinsonian non-human primates resulted in high EI, while driving the model with GPi activity recorded during therapeutic DBS resulted in a lower EI (61). However, these correlations do not necessitate that the EI is a direct measure of motor performance, but rather that there is a strong correlation between the effects of DBS on EI and motor symptoms (61).

Selective pressure toward more fit patterns was exerted using a roulette wheel parent selection process (62) that gave parents with greater fitness a better chance to mate and pass their genes to the next generation. Patterns were numbered from high to low fitness, and parents were selected by iteratively selecting pairs of numbers from an exponential distribution with mean equal to half the population size. One-point crossover was employed to exchange genetic material between the parents and to generate two offspring patterns of stimulation as part of the next generation of patterns. After the offspring were generated, 0.1% of their binary string elements were randomly chosen and switched to mimic genetic mutation. Of the 150 patterns in each generation, 130 were children of the previous generation, 10 were randomly generated immigrants incorporated to add genetic diversity and prevent convergence to local minima, and 10 were the most fit patterns from the previous generation included to assure that optimal patterns were maintained in subsequent generations.

Experimental Testing in Hemi-Parkinsonian Rats

Experiments were conducted in female Long Evans rats weighing 250–350 g. Platinum-iridium stimulation electrode arrays (2×2, 10 kΩ, MicroProbe, Inc.) were implanted under isoflurane (1–3%) anesthesia into the STN using stereotactic technique and acute, single channel intraoperative recordings to guide placement (A: −3.6 mm; L: 2.6 mm; V: −6.8 mm, relative to Bregma, (63)). Rats were rendered hemi-parkinsonian by injection of 6-OHDA into the median forebrain bundle (A: −2.0 mm; L: 2.0 mm; V: −7.0 mm) via a cannula implanted during the preceding electrode implantation surgery. Desipramine (5 mg/kg, i.p.) and pargyline (50 mg/kg, i.p.) were injected 30 min prior to 6-OHDA lesion to limit its non-specific neurotoxic effects (64) and to maximize the toxic effects of 6-OHDA on dopaminergic neurons (65).

Four STN DBS conditions (off, 45 Hz, 130 Hz, GA) were evaluated in the hemi-parkinsonian rats using two independent, unbiased, and quantitative outcome measures to evaluate the effects of the temporal pattern of DBS: the bar test and methamphetamine-induced circling. 130 Hz produces maximal reduction of parkinsonian symptoms in rats; however, in contrast to human, increasing the frequency to 185 Hz in rats is more likely to produce side effects including dyskinesia-like movements (24, 25), and thus lower frequency regular DBS (130 Hz) was used in rats than in humans (185 Hz). All patterns used symmetric, 90 μs per phase biphasic pulses. Stimulation patterns were generated using

MATALB scripts and output through an isolated voltage-to-current convertor (A-M Systems, Analog Stimulus Isolator Model 2200) and a custom AC coupler.

Bar Test

The bar test is a well-established method to quantify akinesia and rigidity in hemi-parkinsonian rats (66, 67). Rats were injected with haloperidol—a long-acting, non-specific dopamine receptor antagonist—and placed in a clear box containing a bar 10 cm above the floor. The forepaws were placed on the bar and the amount of time before the rat dismounted from this unnatural position was recorded as a measure of akinesia. Non-lesioned and drug-naive control animals dismounted the bar in 6.4±2.6 s (mean ± s.e.m.; n=4). Haloperidol doses (0.5–5.0 mg/kg, i.p.) were titrated for each rat to a dose that resulted in the rat staying on the bar for over 5 min (24). Rats were allowed to grip the bar for a maximum of 5 min per trial, and trials started every 10 min following injection. Three trials were performed to confirm the akinetic effect after haloperidol injection, then 30 min of continuous stimulation was applied, and the time required to dismount the bar was recorded and summed across three trials. Experiments testing the different stimulation patterns were carried out on non-consecutive days under the same conditions.

Methamphetamine-Induced Circling

Methamphetamine-induced circling is a well-established method for evaluating locomotor behavior in hemi-parkinsonian rats (68), and exhibits DBS frequency-dependent rescue of ipsiversive circling behavior that parallels frequency-dependent suppression of motor symptoms observed in clinical studies (25). Methamphetamine (1.25–2.5 mg/kg, i.p.) was administered to the rat, and it was placed in a dark cylindrical chamber. An infrared camera and behavioral analysis software (Clever Sys, Inc.) recorded and quantified the rat's rotational asymmetry. Stimulation patterns were presented in randomized order within each block. Four to ten consecutive blocks were run with each rat. Angular velocity and linear speed were quantified for each one-minute epoch of stimulation across patterns and normalized by the angular velocity and linear speed during one minute epochs just prior to and just after the DBS on condition.

Field Potential Recordings in Rats

We implanted stainless steel screws over motor cortex and microwire electrodes in globus pallidus to record field potentials during DBS (n=3). Platinum-iridium electrode arrays (2×2, 10 kΩ, MicroProbe) were implanted ipsilateral to the STN stimulating electrodes under isoflurane (1–3%) anesthesia into the GP using stereotactic technique (A: −1.0 mm; L: 3.0 mm; V: −5.2 mm, relative to Bregma, (63)). 1 mm diameter stainless steel screws were positioned juxtaposed to the dura over ipsilateral motor cortex (A: 2.5 mm; L: 2.5 mm (n=2), or A: 4.5 mm; L: 2.0 mm (n=1) relative to Bregma, (63)). All recordings of neural activity were referenced to titanium screws inserted through the skull over the cerebellum. After recovering from surgery and the 6-OHDA lesioning procedure described above, the rats were placed in a Faraday cage and neural signals were recorded in the freely moving animal. Recordings for each rat took place over the course of 27 min: 9 min for each stimulation condition divided into 3 min pre-, during-, and post-stimulation epochs. Field potential recordings were band-passed filtered (0.7 Hz-300 Hz, 2 poles and 4 poles respectively) and

amplified 5000× before digital sampling at 2 kHz (Plexon MAP System). Multitaper spectral estimates were obtained using the Chronux neural signal analysis package (www.chronux.org) and MATLAB.

Histology

Rats were deeply anesthetized with sodium pentobarbital and killed via intracardiac perfusion with 4% paraformaldehyde. Brains were removed, post-fixed, sucrose-protected, and sectioned coronally with 50 μm thickness. Tyrosine hydroxylase immunochemistry was used to confirm effectiveness of unilateral 6-OHDA lesion (Fig. S4A). Cresyl violet and cytochrome oxidase staining were used to determine electrode placement, and only rats with stimulating electrodes placed in the STN were included in the analysis (Fig. S4B).

Motor Symptom Evaluation in Persons with Parkinson's Disease

The Institutional Review Boards at Duke University and Emory University approved the study protocol, and subjects participated on a volunteer basis following written informed consent. Inclusion criteria were that the subject was at least three months post DBS electrode implant, capable of performing a simple motor evaluation task, neurologically stable, and capable of understanding the study and consent form. Seventeen subjects were consented for the study. Three subjects did not complete the experimental protocol; 5 subjects failed to exhibit better performance during high frequency DBS compared to baseline (DBS off) and were excluded from analysis; one subject's data was discarded due to an inability to confirm that stimulation was delivered; and 8 subjects completed the protocol and were analyzed. Subjects were asked to withhold PD medications for 12 hours prior to surgery, and most (6/8) complied.

Intraoperative Stimulation Protocol and Motor Performance Measurements

The IPG replacement surgery was performed under local anesthetic (lidocaine). Following removal and disconnection of the depleted IPG, a sterile connection was made between the extension cable and the signal generation equipment (20, 69). We quantified motor symptoms unilaterally in subjects with PD—either bradykinesia or tremor—across four conditions: off, 45 Hz, 185 Hz and GA. Although prior studies indicated no difference in the effects of DBS on tremor, rigidity or bradykinesia between 130 Hz and 185 Hz (8, 11, 32), all subjects were programmed to 185 Hz (using their optimal electrode contact pattern) for testing to avoid different control frequencies across subjects. Following completion of the motor symptom evaluation task, the sterile connection between the extension cable and the signal generation equipment was disengaged, and the IPG replacement surgery was completed.

Bradykinesia was quantified in bradykinesia-dominant PD subjects using an alternating finger tapping task (27, 70–73), as the time and physical constraints of the intraoperative environment did not allow the use of the UPDRS to assess outcomes. The hand contralateral to stimulation was placed on a two-button computer mouse, and the subject was instructed to press alternately the buttons as regularly and as rapidly as possible during 20 s trials. Trials were repeated three times during each 5 min stimulation on or stimulation off epoch, but only the two late trials—starting approximately 210 s or 270 s into the 5 min epoch—were

analyzed to account for the time course of the effects of DBS on motor symptoms (74, 75). Analyses including the early trial are included in the Supplementary Material (Fig. S5). After the *baseline* condition, the order of stimulation pattern presentation was randomized, and subjects were blinded to the stimulation conditions. The log-transformed coefficient of variation of tap duration is more strongly correlated with the UPDRS motor score than tapping rate, particularly with the bradykinesia subscore (27), and was used as the outcome measure for bradykinesia across stimulation conditions (20). To estimate the clinical impact of the different patterns of stimulation, changes from baseline in Log CV Duration for each patient were scaled by the gain from the significant correlation between UPDRS part III scores and Log CV Duration (80 UPDRS motor points per 0.75 log units) to predict stimulation-induced changes in UPDRS motor examination scores across stimulation patterns (18, 20, 27).

Experiments in tremor-dominant PD subjects were performed using an accelerometer taped to the dorsum of the subject's hand and a randomized block design with 3 blocks and 1 min stimulation-on/1 min stimulation-off pairs. During 20 s trials, the subject was instructed to maintain their hand in a fixed position and refrain from voluntary movements. Signals from the three accelerometer axes (x, y, z) were detrended using a linear regression based local detrending algorithm (2 s window, 1 s step size), and power spectra were estimated using Welch's method with a 1 s Hanning window and 50% window overlap and summed across all three axes. The peak tremor frequency was between 4–5 Hz, and we quantified tremor by integrating the power between 2–20 Hz to capture the primary peak as well as the first three harmonics. The change in log-transformed power between 2–20 Hz was calculated for each stimulation off/on pair, averaged across blocks, and used as the outcome measure for tremor across stimulation conditions.

To estimate the clinical impact of different stimulation patterns on tremor, we calculated changes in five-point TRS scores between off/on stimulation pairs using:

$$\Delta \mathrm{TRS} = \frac{1}{\alpha} \log\left(\frac{\mathrm{T}_2}{\mathrm{T}_1}\right),$$

where T is tremor amplitude, ΔTRS is the change in tremor rating scale score, and α is an empirically derived linear correlation coefficient (conservatively, α=0.4; (29)). Tremor amplitude is proportional to the square root of the tremor acceleration power. Therefore, we used the square root of the 2–20 Hz tremor power (described above) as a proxy for tremor amplitude and calculated the change in TRS score across patterns.

Intraoperative STN Field Potential Recordings in Subjects with Parkinson's Disease

Field potentials were recorded from the STN in a separate cohort of nine subjects during DBS lead implant surgery, rather than during IPG replacement surgery, using instrumentation described elsewhere (76). Three additional subjects were consented for the study but withdrew before any intraoperative recordings were performed. All subjects were off medications for Parkinson's disease for at least 12 hours prior to surgery.

The recording instrumentation consisted of battery-powered low-noise voltage pre-amplifiers (SR560, Stanford Research Systems) with amplifier blanking in a serial configuration with diode clamps between stages (76). The relay at the stimulator that disconnected the stimulating contact between pulses, as described in (76), was removed, and the amplifiers were blanked between 20 μs before through 20–500 μs after each DBS pulse, which allowed sufficient gain (2,000–10,000×) for field potential recordings without saturation. Although the stimulation waveforms and patterns were the same across all subjects, the duration of stimulation artifacts were variable, apparently as a result of differences in the tissue properties around the electrodes (77). Therefore, the amplifier blanking duration was tuned individually for each patient.

Symmetric biphasic pulses (90 μs per phase) were delivered through contact 1 or 2 on the DBS electrode lead (whichever was determined to be clinically effective by the attending neurologist), and the stimulation counter electrode was placed on the chest (StimCare Carbon Foam Electrode, Empi). Bipolar recordings were made from contacts 0 and 2 (0+/2−) or contacts 1 and 3 (1+/3−) on the DBS electrode lead, and the implanted cannula served as the recording reference electrode. The 4-contact lead is implanted to place at least 2 contacts (typically 1 and 2 but occasionally 0 and 1) within the T2-positive region considered to be subthalamic nucleus on MR imaging (fusing the postoperative CT scan with the pre-operative MRI scan), and electrode tracks were located within the STN with > 4 mm electrode track depth of STN. Stimulation was delivered at an amplitude determined to be effective by the neurologist performing the intraoperative assessment (1.5–3.0 V). 45 Hz, GA, and 130 Hz were presented in randomized order for 60 s (n=4) or 300 s (n=5) intervals with intervening intervals of no stimulation. One subject received only 130 Hz before withdrawing and was excluded from analysis.

Our objective was to quantify the effects of DBS on ongoing β-band activity, as prior data suggested that this activity is correlated with bradykinesia in PD (34, 35) and changes in response to DBS in a manner that paralleled the changes in symptoms (36). The field potential data were high-pass filtered to remove offset and very slow signal components (2 Hz cutoff, 3 pole Butterworth filter, MATLAB), and the signal was smoothed around the amplifier blanking epoch by linear interpolation from 0.1 ms before to 1.5 ms after the start of the DBS pulse. Evoked compound action potentials were observed in the interpulse intervals (77), and the averaged evoked response was subtracted from the signal to reduce spectral power at the stimulation frequency. Finally, the data were band-pass filtered between 2–100 Hz and down-sampled to 400 Hz before spectral analysis (chronux.org). The final 20 s or 95 s of data from the 60 s and 300 s trials for each condition was selected for spectral analysis (except in one subject who did not complete 300 s of data collection for 130 Hz and a 15 s trial was used in its place). β power was quantified as the percentage of power in a 14 Hz window centered around the β peak in the OFF condition. Two subjects were excluded from analysis because they did not have a prominent β peak in the OFF condition (defined as < 1%/Hz peak power in a β band), leaving six subjects included in the analysis. In most subjects this window coincided well with the high β range (20–33 Hz). However, in one subject the β peak was at 14 Hz, and the window was contracted so that it did not include frequencies below 10 Hz.

The data processing methods did not artificially reduce β power in the recorded field potentials for the GA condition. In fact, the two subjects that did not have β peaks in their field potential spectra had increased β power due to the GA pattern data processing methods, which introduced small spectral artifacts in the β range (Fig. S6).

Statistical Analysis

Finger-tapping and tremor data were collected using LabVIEW and processed in MATLAB. Technical outliers were removed from the mouse clicking data by discarding extremely short clicks that were artifacts of the computer mouse clicking apparatus (debouncing; visual inspection of click duration histograms; Fig. S7). Statistical analyses were conducted in StatView 5.0.1 for Windows. All rat and human data were analyzed using repeated measures analysis of variance (ANOVA). *Post-hoc* comparisons between stimulation patterns were performed when indicated by the repeated measures ANOVA using the Fisher's protected least significant difference test (PLSD) with significance defined at $\alpha=0.05$.

Supplementary Material

Refer to Web version on PubMed Central for supplementary material.

Acknowledgments

We thank G. Mills for laboratory support and A. August for assistance with histology.

Funding: This work was supported by NIH grants R01 NS040894, R37 NS040894, and R01 NS079312.

References and Notes

1. Gelb DJ, Oliver E, Gilman S. Diagnostic criteria for Parkinson disease. Arch Neurol. 1999; 56:33–39. [PubMed: 9923759]
2. Hughes AJ, Daniel SE, Kilford L, Lees AJ. Accuracy of clinical diagnosis of idiopathic Parkinson's disease: a clinico-pathological study of 100 cases. J Neurol Neurosurg Psychiatry. 1992; 55:181–184. [PubMed: 1564476]
3. Lesser RP, Fahn S, Snider SR, Cote LJ, Isgreen WP, Barrett RE. Analysis of the clinical problems in parkinsonism and the complications of long-term levodopa therapy. Neurology. 1979; 29:1253–1253. [PubMed: 573405]
4. Benabid AL, Chabardes S, Mitrofanis J, Pollak P. Deep brain stimulation of the subthalamic nucleus for the treatment of Parkinson's disease. Lancet Neurol. 2009; 8:67–81. [PubMed: 19081516]
5. Moro E, Lozano AM, Pollak P, Agid Y, Rehncrona S, Volkmann J, Kulisevsky J, Obeso JA, Albanese A, Hariz MI. Long-term results of a multicenter study on subthalamic and pallidal stimulation in Parkinson's disease. Mov Disord. 2010; 25:578–586. [PubMed: 20213817]
6. Weaver FM, Follett K, Stern M, Hur K, Harris C, Marks WJ Jr, Rothlind J, Sagher O, Reda D, Moy CS. Bilateral deep brain stimulation vs best medical therapy for patients with advanced Parkinson disease. JAMA. 2009; 301:63–73. [PubMed: 19126811]
7. Benabid A, Pollak P, Gross C, Hoffmann D, Benazzouz A, Gao D, Laurent A, Gentil M, Perret J. Acute and long-term effects of subthalamic nucleus stimulation in Parkinson's disease. Stereotact Funct Neurosurg. 1994; 62:76–84. [PubMed: 7631092]
8. Limousin P, Pollak P, Benazzouz A, Hoffmann D, Le Bas JF, Broussolle E, Perret JE, Benabid AL, Broussolle E. Effect on parkinsonian signs and symptoms of bilateral subthalamic nucleus stimulation. Lancet. 1995; 345:91–95. [PubMed: 7815888]

9. Siegfried J, Lippitz B. Bilateral chronic electrostimulation of ventroposterolateral pallidum: a new therapeutic approach for alleviating all parkinsonian symptoms. Neurosurgery. 1994; 35:1126–1129. [PubMed: 7885558]
10. Kuncel AM, Cooper SE, Wolgamuth BR, Clyde MA, Snyder SA, Montgomery EB Jr, Rezai AR, Grill WM. Clinical response to varying the stimulus parameters in deep brain stimulation for essential tremor. Mov Disord. 2006; 21:1920–1928. [PubMed: 16972236]
11. Rizzone M, Lanotte M, Bergamasco B, Tavella A, Torre E, Faccani G, Melcarne A, Lopiano L. Deep brain stimulation of the subthalamic nucleus in Parkinson's disease: effects of variation in stimulation parameters. J Neurol Neurosurg Psychiatry. 2001; 71:215–219. [PubMed: 11459896]
12. Koss AM, Alterman RL, Tagliati M, Shils JL. Calculating total electrical energy delivered by deep brain stimulation systems. Ann Neurol. 2005; 58:168. [PubMed: 15984018]
13. Bin-Mahfoodh M, Hamani C, Sime E, Lozano AM. Longevity of batteries in internal pulse generators used for deep brain stimulation. Stereotact Funct Neurosurg. 2003; 80:56–60. [PubMed: 14745210]
14. Pepper J, Zrinzo L, Mirza B, Foltynie T, Limousin P, Hariz M. The Risk of Hardware Infection in Deep Brain Stimulation Surgery Is Greater at Impulse Generator Replacement than at the Primary Procedure. Stereotact Funct Neurosurg. 2013; 91:56–65. [PubMed: 23207787]
15. Baker KB, Zhang J, Vitek JL. Pallidal stimulation: Effect of pattern and rate on bradykinesia in the non-human primate model of Parkinson's disease. Exp Neurol. 2011; 231:309–313. [PubMed: 21767534]
16. Rosin B, Slovik M, Mitelman R, Rivlin-Etzion M, Haber SN, Israel Z, Vaadia E, Bergman H. Closed-loop deep brain stimulation is superior in ameliorating parkinsonism. Neuron. 2011; 72:370–384. [PubMed: 22017994]
17. McConnell GC, So RQ, Grill WM. Failure to suppress low-frequency neuronal oscillatory activity underlies the reduced effectiveness of random patterns of deep brain stimulation. J Neurophysiol. 2016
18. Dorval AD, Kuncel AM, Birdno MJ, Turner DA, Grill WM. Deep brain stimulation alleviates parkinsonian bradykinesia by regularizing pallidal activity. J Neurophysiol. 2010; 104:911–921. [PubMed: 20505125]
19. Montgomery E Jr. Effect of subthalamic nucleus stimulation patterns on motor performance in Parkinson's disease. Parkinsonism Relat Disord. 2005; 11:167–171. [PubMed: 15823481]
20. Brocker DT, Swan BD, Turner DA, Gross RE, Tatter SB, Miller Koop M, Bronte-Stewart H, Grill WM. Improved efficacy of temporally non-regular deep brain stimulation in Parkinson's disease. Exp Neurol. 2013; 239:60–67. [PubMed: 23022917]
21. Birdno MJ, Kuncel AM, Dorval AD, Turner DA, Grill WM. Tremor varies as a function of the temporal regularity of deep brain stimulation. Neuroreport. 2008; 19:599–602. [PubMed: 18388746]
22. Birdno MJ, Kuncel AM, Dorval AD, Turner DA, Gross RE, Grill WM. Stimulus features underlying reduced tremor suppression with temporally patterned deep brain stimulation. J Neurophysiol. 2012; 107:364–83. [PubMed: 21994263]
23. Rubin JE, Terman D. High Frequency Stimulation of the subthalamic nucleus eliminates pathological thalamic rhythmicity in a computational model. J Comput Neurosci. 2004; 16:211–235. [PubMed: 15114047]
24. McConnell GC, So RQ, Hilliard JD, Lopomo P, Grill WM. Effective deep brain stimulation suppresses low-frequency network oscillations in the basal ganglia by regularizing neural firing patterns. J Neurosci. 2012; 32:15657–15668. [PubMed: 23136407]
25. So RQ, McConnell GC, August A, Grill WM. Characterizing effects of subthalamic nucleus deep brain stimulation on methamphetamine-induced circling behavior in hemi-parkinsonian rats. IEEE Trans Neural Syst Rehabil Eng. 2012; 20:626–635. [PubMed: 22692937]
26. Li Q, Ke Y, Chan DC, Qian ZM, Yung KK, Ko H, Arbuthnott GW, Yung WH. Therapeutic deep brain stimulation in Parkinsonian rats directly influences motor cortex. Neuron. 2012; 76:1030–41. [PubMed: 23217750]
27. Taylor Tavares AL, Jefferis GSXE, Koop M, Hill BC, Hastie T, Heit G, Bronte-Stewart HM. Quantitative measurements of alternating finger tapping in Parkinson's disease correlate with

UPDRS motor disability and reveal the improvement in fine motor control from medication and deep brain stimulation. Mov Disord. 2005; 20:1286–1298. [PubMed: 16001401]

28. Hamani C, Richter E, Schwalb JM, Lozano AM. Bilateral subthalamic nucleus stimulation for Parkinson's disease: a systematic review of the clinical literature. Neurosurgery. 2005; 56:1313–1324. [PubMed: 15918948]
29. Elble RJ, Pullman SL, Matsumoto JY, Raethjen J, Deuschl G, Tintner R. Tremor amplitude is logarithmically related to 4-and 5-point tremor rating scales. Brain. 2006; 129:2660–2666. [PubMed: 16891320]
30. Brown P. Abnormal oscillatory synchronisation in the motor system leads to impaired movement. Curr Opin Neurobiol. 2007; 17:656–664. [PubMed: 18221864]
31. Fogelson N, Kuhn AA, Silberstein P, Limousin PD, Hariz M, Trottenberg T, Kupsch A, Brown P. Frequency dependent effects of subthalamic nucleus stimulation in Parkinson's disease. Neurosci Lett. 2005; 382:5–9. [PubMed: 15911112]
32. Moro E, Esselink RJA, Xie J, Hommel M, Benabid AL, Pollak P. The impact on Parkinson's disease of electrical parameter settings in STN stimulation. Neurology. 2002; 59:706–713. [PubMed: 12221161]
33. Ray N, Jenkinson N, Wang S, Holland P, Brittain J, Joint C, Stein J, Aziz T. Local field potential beta activity in the subthalamic nucleus of patients with Parkinson's disease is associated with improvements in bradykinesia after dopamine and deep brain stimulation. Exp Neurol. 2008; 213:108–113. [PubMed: 18619592]
34. Kühn AA, Kupsch A, Schneider GH, Brown P P. Reduction in subthalamic 8–35 Hz oscillatory activity correlates with clinical improvement in Parkinson's disease. Eur J Neurosci. 2006; 23:1956–1960. [PubMed: 16623853]
35. Pogosyan A, Yoshida F, Chen CC, Martinez-Torres I, Foltynie T, Limousin P, Zrinzo L, Hariz MI, Brown P. Parkinsonian impairment correlates with spatially extensive subthalamic oscillatory synchronization. Neuroscience. 2010; 171:245–257. [PubMed: 20832452]
36. Eusubio A, Cagnan H, Brown P P. Does suppression of oscillatory synchronization mediate some of the therapeutic effects of DBS in patients with Parkinson's disease. Front Int Neurosci. 2012; 6:1–9.
37. Weinberger M, Mahant N, Hutchison WD, Lozano AM, Moro E, Hodaie M, Lang AE, Dostrovsky JO. Beta oscillatory activity in the subthalamic nucleus and its relation to dopaminergic response in Parkinson's disease. J Neurophysiol. 2006; 96:3248–3256. [PubMed: 17005611]
38. Rosa M, Giannicola G, Servello D, Marceglia S, Pacchetti C, Porta M, Sassi M, Scelzo E, Barbieri S, Priori A. Subthalamic local field beta oscillations during ongoing deepbrain stimulation in Parkinson's disease in hyperacute and chronicphases. Neurosignals. 2011; 19:151–162. [PubMed: 21757872]
39. Priori A, Foffani G, Rossi L, Marceglia S. Adaptive deep brain stimulation (aDBS) controlled by local field potential oscillations. Exp Neurol. 2013; 245:77–86. [PubMed: 23022916]
40. Ondo WG, Meilak C, Vuong KD. Predictors of battery life for the Activa® Soletra 7426 Neurostimulator. Parkinsonism Relat Disord. 2007; 13:240–242. [PubMed: 17379565]
41. Tsang E, Hamani C, Moro E, Mazzella F, Saha U, Lozano A, Hodaie M, Chuang R, Steeves T, Lim S. Subthalamic deep brain stimulation at individualized frequencies for Parkinson disease. Neurology. 2012; 78:1930–1938. [PubMed: 22592373]
42. Kuncel AM, Birdno MJ, Swan BD, Grill WM. Tremor reduction and modeled neural activity during cycling thalamic deep brain stimulation. Clin Neurophysiol. 2012; 123:1044–1052. [PubMed: 21978653]
43. Swan BD, Brocker DT, Hilliard JD, Tatter SB, Gross RE, Turner DA, Grill WM. Short pauses in thalamic deep brain stimulation promote tremor and neuronal bursting. Clin Neurophysiol. 2016; 127:1551–1559. [PubMed: 26330131]
44. Volkmann J, Herzog J, Kopper F, Deuschl G. Introduction to the programming of deep brain stimulators. Mov Disord. 2002; 17:S181–S187. [PubMed: 11948775]
45. Beuter A, Titcombe MS. Modulation of tremor amplitude during deep brain stimulation at different frequencies. Brain and Cognition. 2003; 53:190–192. [PubMed: 14607145]

46. Lopiano L, Torre E, Benedetti F, Bergamasco B, Perozzo P, Pollo A, Rizzone M, Tavella A, Lanotte M. Temporal changes in movement time during the switch of the stimulators in Parkinson's disease patients treated by subthalamic nucleus stimulation. Eur Neurol. 2003; 50:94–99. [PubMed: 12944714]
47. Krack P, Batir A, Van Blercom N, Chabardes S, Fraix V, Ardouin C, Koudsie A, Limousin PD, Benazzouz A, LeBas JF, Benabid AL, Pollak P. Five-year follow-up of bilateral stimulation of the subthalamic nucleus in advanced Parkinson's disease. N Engl J Med. 2003; 349:1925–1934. [PubMed: 14614167]
48. Deuschl G, Schade-Brittinger C, Krack P, Volkmann J, Schäfer H, Bötzel K, Daniels C, Deutschländer A, Dillmann U, Eisner W, Gruber D, Hamel W, Herzog J, Hilker R, Klebe S, Kloss M, Koy J, Krause M, Kupsch A, Lorenz D, Lorenzl S, Mehdorn HM, Moringlane JR, Oertel W, Pinsker MO, Reichmann H, Reuss A, Schneider GH, Schnitzler A, Steude U, Sturm V, Timmermann L, Tronnier V, Trottenberg T, Wojtecki L, Wolf E, Poewe W, Voges J. German Parkinson Study Group, Neurostimulation Section, A randomized trial of deep-brain stimulation for Parkinson's disease. N Engl J Med. 2006; 355:896–908. [PubMed: 16943402]
49. Follett KA, Weaver FM, Stern M, Hur K, Harris CL, Luo P, Marks WJ, Rothlind J, Sagher O, Moy C, Pahwa R, Burchiel K, Hogarth P, Lai EC, Duda JE, Holloway K, Samii A, Horn S, Bronstein JM, Stoner G, Starr PA, Simpson R, Baltuch G, De Salles A, Huang GD, Reda DJ. CSP 468 Study Group, Pallidal versus subthalamic deep-brain stimulation for Parkinson's disease. N Engl J Med. 2010; 362:2077–2091. [PubMed: 20519680]
50. Schrag A, Sampaio C, Counsell N, Poewe W. Minimal clinically important change on the unified Parkinson's disease rating scale. Mov Disord. 2006; 21:1200–1207. [PubMed: 16673410]
51. Shulman LM, Gruber-Baldini AL, Anderson KE, Fishman PS, Reich SG, Weiner WJ. The clinically important difference on the unified Parkinson's disease rating scale. Arch Neurol. 2010; 67:64–70. [PubMed: 20065131]
52. Santaniello S, Fiengo G, Glielmo L, Grill WM. Closed-loop control of deep brain stimulation: a simulation study. IEEE Tans Neural Sys Rehabil Eng. 2011; 19:15–24.
53. Stanslaski S, Afshar P, Cong P, Giftakis J, Stypulkowski P, Carlson D, Linde D, Ullestad D, Avestruz A, Denison T. Design and validation of a fully implantable, chronic, closed-loop neuromodulation device with concurrent sensing and stimulation. IEEE Tans Neural Sys Rehabil Eng. 2012; 20:410–421.
54. So RQ, Kent AR, Grill WM. Relative contributions of local cell and passing fiber activation and silencing to changes in thalamic fidelity during deep brain stimulation and lesioning: a computational modeling study. J Comput Neurosci. 2012; 32:499–519. [PubMed: 21984318]
55. Bergman H, Wichmann T, Karmon B, DeLong M. The primate subthalamic nucleus. II. Neuronal activity in the MPTP model of parkinsonism. J Neurophysiol. 1994; 72:507–520. [PubMed: 7983515]
56. Starr P, Rau G, Davis V, Marks W, Ostrem J, Simmons D, Lindsey N, Turner R. Spontaneous pallidal neuronal activity in human dystonia: comparison with Parkinson's disease and normal macaque. J Neurophysiol. 2005; 93:3165–3176. [PubMed: 15703229]
57. Steigerwald F, Potter M, Herzog J, Pinsker M, Kopper F, Mehdorn H, Deuschl G, Volkmann J. Neuronal activity of the human subthalamic nucleus in the parkinsonian and nonparkinsonian state. J Neurophysiol. 2008; 100:2515–2524. [PubMed: 18701754]
58. Wichmann T, Soares J. Neuronal firing before and after burst discharges in the monkey basal ganglia is predictably patterned in the normal state and altered in parkinsonism. J Neurophysiol. 2006; 95:2120–2133. [PubMed: 16371459]
59. Cagnan H, Meijer HGE, Van Gils SA, Krupa M, Heida T, Rudolph M, Wadman WJ, Martens HCF. Frequency-selectivity of a thalamocortical relay neuron during Parkinson's disease and deep brain stimulation: a computational study. Eur J Neurosci. 2009; 30:1306–1317. [PubMed: 19788577]
60. Guo Y, Rubin JE. Multi-site stimulation of subthalamic nucleus diminishes thalamocortical relay errors in a biophysical network model. Neural Netw. 2011; 24:602–616. [PubMed: 21458952]
61. Guo Y, Rubin JE, McIntyre CC, Vitek JL, Terman D. Thalamocortical relay fidelity varies across subthalamic nucleus deep brain stimulation protocols in a data-driven computational model. J Neurophysiol. 2008; 99:1477–1492. [PubMed: 18171706]

62. Davis, L. Handbook of genetic algorithms. Davis, L., editor. Van Nostrand Reinhold; New York: 1991.
63. Paxinos, G., Watson, C. The Rat Brain in Stereotaxic Coordinates: Hard Cover Edition. 6. Academic press; 2007.
64. Lin M, Kao T, Chio C, Jin Y. Dopamine depletion protects striatal neurons from heatstroke-induced ischemia and cell death in rats. Am J Physiol. 1995; 269:H487–H490. [PubMed: 7653613]
65. Schwarting R, Huston J. Unilateral 6-hydroxydopamine lesions of meso-striatal dopamine neurons and their physiological sequelae. Prog Neurobiol. 1996; 49:215–266. [PubMed: 8878304]
66. Duvoisin R. Parkinsonism: animal analogues of the human disorder. Res Publ Assoc Res Nerv Ment Dis. 1976; 55:293–303. [PubMed: 826997]
67. Sanberg PR, Bunsey MD, Giordano M, Norman AB. The catalepsy test: Its ups and downs. Behav Neurosci. 1988; 102:748–759. [PubMed: 2904271]
68. Ungerstedt U, Arbuthnott GW. Quantitative recording of rotational behavior in rats after 6-hydroxy-dopamine lesions of the nigrostriatal dopamine system. Brain Res. 1970; 24:485–493. [PubMed: 5494536]
69. Swan BD, Grill WM, Turner DA. Investigation of deep brain stimulation mechanisms during implantable pulse generator replacement surgery. Neuromodulation. 2014; 17:419–424. [PubMed: 24118257]
70. Burns B, DeJong J. A preliminary report on the measurement of Parkinson's disease. Neurology. 1960; 10:1096–1102. [PubMed: 13689185]
71. Giovannoni G, Van Schalkwyk J, Fritz V, Lees A. Bradykinesia akinesia inco-ordination test (BRAIN TEST): an objective computerised assessment of upper limb motor function. J Neurol Neurosurg Psychiatry. 1999; 67:624–629. [PubMed: 10519869]
72. Homann CN, Suppan K, Wenzel K, Giovannoni G, Ivanic G, Horner S, Ott E, Hartung HP. The bradykinesia akinesia incoordination test (BRAIN TEST), an objective and user-friendly means to evaluate patients with Parkinsonism. Mov Disord. 2000; 15:641–647. [PubMed: 10928573]
73. Pal P, Lee C, Samii A, Schulzer M, Stoessl A, Mak E, Wudel J, Dobko T, Tsui J. Alternating two finger tapping with contralateral activation is an objective measure of clinical severity in Parkinson's disease and correlates with PET. Parkinsonism Relat Disord. 2001; 7:305–309. [PubMed: 11344014]
74. Temperli P, Ghika J, Villemure JG, Burkhard PR, Bogousslavsky J, Vingerhoets FJG. How do parkinsonian signs return after discontinuation of subthalamic DBS? Neurology. 2003; 60:78–81. [PubMed: 12525722]
75. Waldau B, Clayton D, Gasperson L, Turner D. Analysis of the time course of the effect of subthalamic nucleus stimulation upon hand function in Parkinson's patients. Stereotact Funct Neurosurg. 2011; 89:48–55. [PubMed: 21252589]
76. Kent AR, Grill WM. Recording evoked potentials during deep brain stimulation: development and validation of instrumentation to suppress the stimulus artefact. J Neural Eng. 2012; 9:036004. [PubMed: 22510375]
77. Kent AR, Swan BD, Brocker DT, Turner DA, Gross RE, Grill WM. Measurement of evoked potentials during thalamic deep brain stimulation. Brain Stimul. 2014; 8:42–56. [PubMed: 25457213]

One Sentence Summary

Model-based computational evolution was used to design a novel temporal pattern of brain stimulation that required substantially less energy to reduce symptoms in a parkinsonian animal model and in persons with Parkinson's disease.

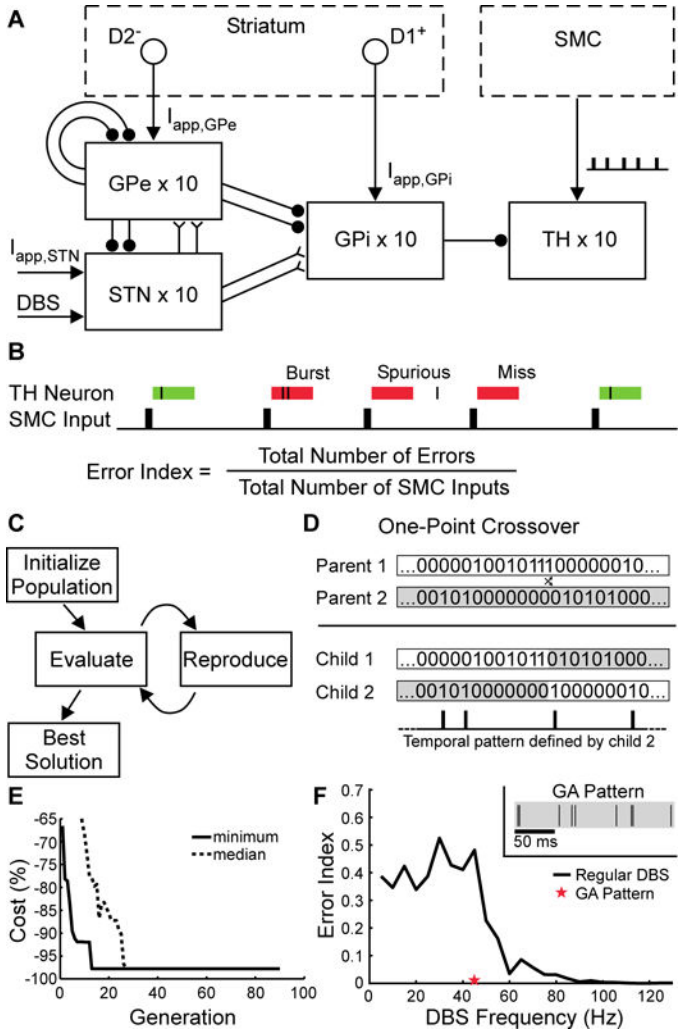

Fig. 1.

Model-based design by computational evolution of an optimized temporal pattern of DBS. (**A**) Computational model of the parkinsonian basal ganglia that included the external globus pallidus (GPe), subthalamic nucleus (STN), internal globus pallidus (GPi), thalamus (TH), and an input action potential train from the sensorimotor cortex (SMC). Applied currents (→) representing inputs to GPe, GPi, and STN were modeled ($I_{app,GPe}$, $I_{app,GPi}$, and $I_{app,STN}$); GPe primarily receives inputs from striatal neurons expressing inhibitory D2-type receptors ($D2^{-}$), while GPi primarily receives inputs from striatal neurons expressing excitatory D1-type receptors ($D1^{+}$). Excitatory and inhibitory synapses are depicted using forked (Y) and circular (•) terminations. (**B**) The error index (EI), a measure of the fidelity of thalamic neuron response to SMC input. If a thalamic (TH) neuron did not fire an action potential within 25 ms of a SMC input, an error occurred. There were three types of errors: misses, bursts, and spurious. EI was defined as the total number of errors divided by the total number of SMC inputs. (**C**) Diagram of the genetic algorithm. A random population of stimulation patterns was initialized. Subsequent generations of patterns were created by using principles from biological evolution and evaluated according to the cost function. After convergence, the pattern with the lowest cost (GA) was selected to be tested in the

hemi-parkinsonian rats and human patients. (**D**) Representation of stimulation patterns. Defined by binary strings, new patterns were created by one-point crossover. (**E**) Trajectory of convergence to the GA pattern of stimulation during successive generations of modeling. (**F**) Error index of standard (black line) and the optimized GA (red star) stimulation pattern. (Inset) A 200-ms segment of the repeating GA pattern of stimulation.

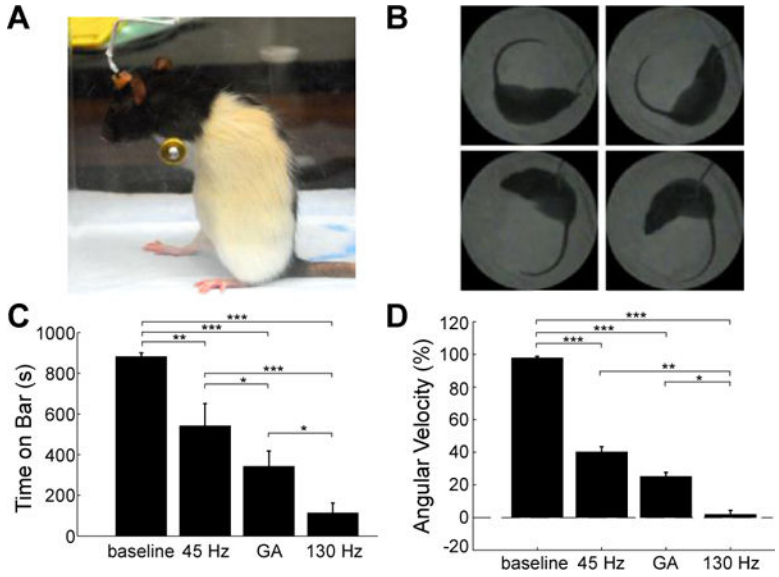

Fig. 2.

Effects of temporal patterns of STN DBS on motor symptoms in hemi-parkinsonian rats evaluated using the bar test (**A**) and methamphetamine-induced circling (**B**). (**C**) Total time (mean ± sem) spent on bar in all three stimulation conditions in the bar test (n=9). Rats were akinetic and unable to dismount from the bar during baseline, but DBS patterns differentially rescued akinesia. (**D**) Normalized circling rate (mean ± sem) across stimulation conditions (n=13). The pathological ipsiversive circling rate was differentially reduced by the DBS patterns. Repeated measures analysis of variance (RM-ANOVA) revealed a significant effect of stimulation condition on time on the bar ($p<0.0001$) and normalized angular velocity ($p<0.0001$). Fisher's protected least significant difference (PLSD) test was used to perform *post-hoc* comparisons between stimulation conditions (*** $p<0.0001$; ** $p<0.001$; * $p<0.05$).

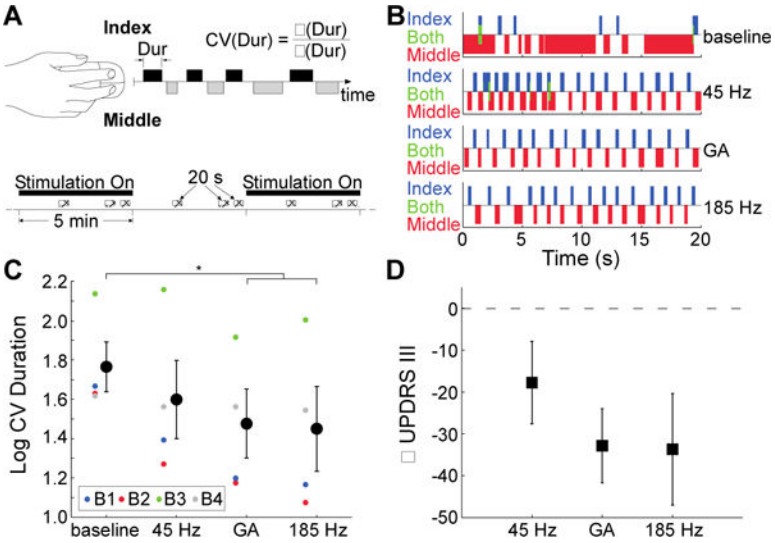

Fig. 3.

Effects of temporal patterns of STN DBS on bradykinesia in persons with PD. (**A**) Diagram of data collection (top) and stimulation schedule (bottom) for evaluation of bradykinesia in PD subjects by using a finger tapping task. Stimulation patterns were applied during the intraoperative experiment with 5 min on-off intervals, and finger tapping data were collected for 20 seconds thrice during each 5 min epoch (crosshatched rectangles). The coefficient of variation (CV) of index finger tap durations (Dur) was calculated as the standard deviation (σ) divided by the mean (μ) of the tap durations. (**B**) Data from subject B1 across the four experimental conditions. (**C**) Coefficient of variation for index finger tap durations (log-transformed) − (mean ± sem) across stimulation conditions. RM-ANOVA revealed a significant effect of stimulation condition on regularity of finger tapping ($p = 0.01$, $n = 4$), and Fisher's PLSD test was used to perform *post-hoc* comparisons between stimulation conditions. GA and 185 Hz DBS significantly improved performance in the finger tapping task relative to baseline ($p = 0.006$ and $p = 0.004$, respectively). Tapping variability was lower for the GA and 185 Hz DBS conditions compared to the 45 Hz DBS condition, but the differences were not statistically significant ($p = 0.17$ and $p = 0.10$, respectively). Individual colored symbols represent individual participants. (**D**) Changes in UPDRS III scores (mean ± sem) from baseline for various stimulation patterns predicted from the finger tapping task data.

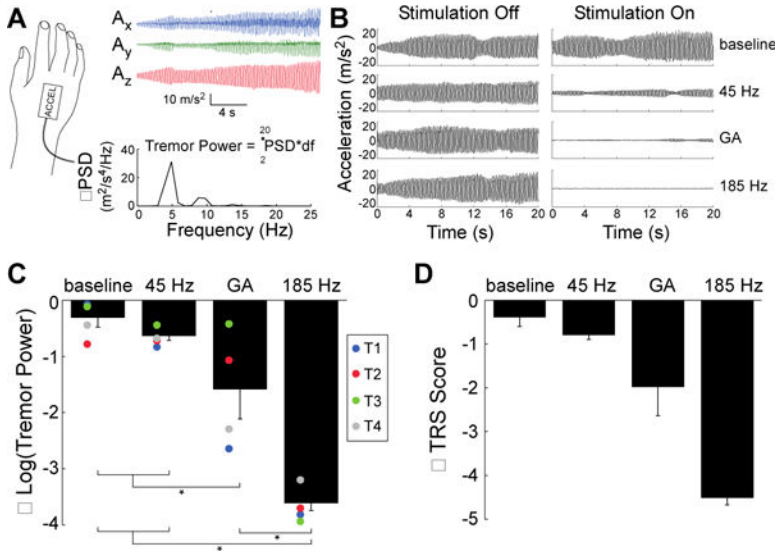

Fig. 4.

Effects of temporal patterns of STN DBS on tremor in persons with PD. (**A**) Tremor was quantified in subjects with tremor-dominant PD by attaching an accelerometer to the dorsum of the hand. The power spectral density (PSD) was estimated and summed across the three orthogonal accelerometer axes (A_x, A_y, A_z), and *tremor power* (m^2/s^4) was calculated by integrating the summed PSD (ΣPSD) with respect to frequency (df) in the 2-20 Hz range. (**B**) Tremor data from subject T1 across the four experimental conditions. (**C**) Changes in mean (± sem) log-transformed tremor power (2–20 Hz) across stimulation conditions, as compared to the stimulation off condition. RM-ANOVA revealed a significant effect of DBS stimulation condition on tremor ($p < 0.0001$, $n = 4$), and Fisher's PLSD test was used to perform *post-hoc* comparisons between stimulation conditions. GA and 185 Hz DBS significantly reduced tremor relative to baseline ($p = 0.01$ and $p < 0.0001$, respectively) and relative to 45 Hz DBS ($p = 0.048$ and $p < 0.0001$, respectively). However, 45 Hz DBS did not significantly reduce tremor relative to baseline ($p = 0.45$). Individual colored symbols represent individual participants. (**D**) Changes in TRS (mean ± SEM) across stimulation conditions predicted from accelerometer measurements, compared to baseline.

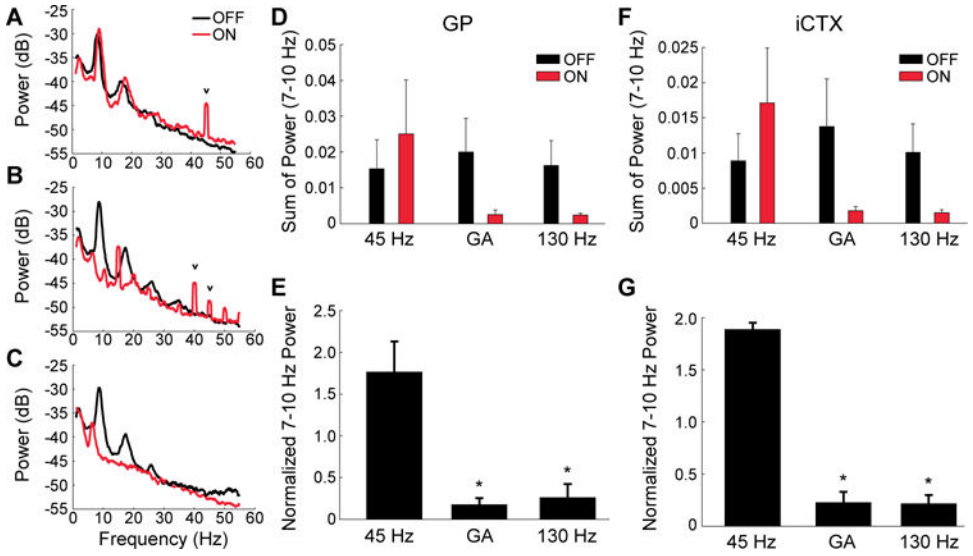

Fig. 5.

Effect of temporal pattern of STN DBS on low-frequency oscillations in the globus pallidus (GP) and ipsilateral cortex (iCTX) of hemi-parkinsonian rats. (**A through C**) Power spectra of local field potentials recorded from the GP during regular 45 Hz (A), GA (B), and regular 130 Hz DBS (C). The small, narrow peaks (v) in the power spectra are residual artifacts from amplifier blanking and signal interpolation to minimize the contribution of stimulation artifacts to the recorded signals. (**D and F**) Sum of 7–10 Hz power (mean ± sem) in the three stimulation conditions in GP (D) and iCTX (F). Low frequency (7–10 Hz) oscillatory power during each DBS pattern was normalized by the pre- and post-stimulation power. (**E and G**) Normalized 7–10 Hz power (mean ± sem) in the three stimulation patterns in GP (E) and iCTX (G). RM-ANOVA revealed a significant effect of DBS condition on normalized 7–10 Hz power in GP ($p = 0.0035$, $n = 3$) and iCTX ($p = 0.0003$, $n = 3$), and Fisher's PLSD test was used to perform *post-hoc* comparisons between stimulation conditions. GA and regular 130 Hz DBS significantly reduced normalized 7–10 Hz power compared to regular 45 Hz DBS in GP ($p = 0.0021$ and $p = 0.0026$, respectively) and in iCTX ($p = 0.0002$).

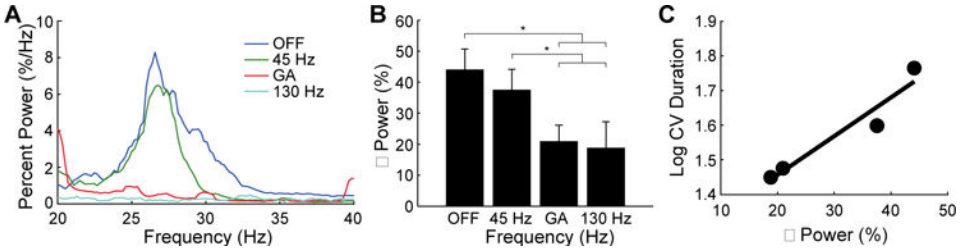

Fig. 6.

Effect of temporal pattern of DBS on β band oscillatory activity in the STN of persons with PD. (**A**) Spectra estimated for the three stimulation conditions. Local field potentials recorded from the STN during DBS lead implant surgery. (**B**) Percent β power quantified across stimulation conditions and averaged across subjects (n=6; mean ± sem). Power in the beta range (typically 20 Hz to 33 Hz) was integrated and compared across stimulation conditions. RM-ANOVA revealed a significant effect of DBS condition on percent β power ($p = 0.0007$), and Fisher's PLSD test was used to perform *post-hoc* comparisons between stimulation conditions. GA DBS and 130 Hz DBS significantly suppressed beta power compared to DBS off ($p = 0.0008$ and $p = 0004$, respectively) and 45 Hz DBS ($p = 0.0092$ and $p = 0.0041$, respectively). (**C**) Relationship between percent β power and finger tapping task performance (as measured by log CV duration). The best fit line is shown for log CV duration data from Fig. 3C and the percent β power data from panel B.

Table 1

Subject information.

	Subject	Age/Sex	Hemisphere/Target Tested	Electrode Contacts[a,b]	AMP (V)[b]	PW (μs)	FREQ (Hz)	PD medications 12 hours prior to surgery
Bradykinesia	B1	55/M	Right/STN	$1^-/2^-/0^+$	3.9	60	185	none
	B2	59/M	Right/STN	$0^-/1^-/2^+$	3.5	60	185	none
	B3	69/F	Left/STN	$1^-/2^-/3^+$ [$1^-/2^-/C^+$]	2.6	60	185	10 mg carbidopa 100 mg levodopa
	B4	64/M	Right/STN	$1^-/2^-/3^+$ [$1^-/2^-/3^-/C^+$]	4.0 [1.9]	60	185	25 mg carbidopa 250 mg levodopa
Tremor	T1	69/M	Right/STN	$1^-/2^-/3^-/0^+$ [$1^-/2^-/3^-/C^+$]	3.5 [3.8]	90	135	none
	T2	66/M	Right/STN	$2^-/3^+$ [$2^-/C^+$]	2.2 [3.3]	60	130	none
	T3	66/M	Right/STN	$1^-/2^-/3^+$ [$1^-/2^-/C^+$]	3.2	60	180	none
	T4	59/F	Left/STN	$1^-/2^-/3^+$	2.5	90	180	none

[a] Quadripolar DBS electrode contacts are numbered 0 through 3, with 0 most distal and 3 most proximal. Contact polarity denoted by '+' (cathode) and '−' (anode). C^+ indicates that the IPG case was used as the anode/current return.

[b] Experimental stimulation parameters are shown. Clinical settings different from the experimental settings are shown in brackets.

Abbreviations: M = male; F = female; AMP = amplitude; PW = pulse width; FREQ = frequency; STN =subthalamic nucleus.